POLITECNICO DI TORINO
Repository ISTITUZIONALE

Gravitomagnetic resonance in the field of a gravitational wave

Original
Gravitomagnetic resonance in the field of a gravitational wave / Ruggiero, M.L., Ortolan, A.. - In: PHYSICAL REVIEW D. - ISSN 2470-0010. - 102:10(2020), p. 101501. [10.1103/PhysRevD.102.101501]

Availability:
This version is available at: 11583/2927356 since: 2021-09-26T12:19:32Z

Publisher:
American Physical Society

Published
DOI:10.1103/PhysRevD.102.101501

Terms of use:

This article is made available under terms and conditions as specified in the corresponding bibliographic description in the repository

Publisher copyright

(Article begins on next page)

26 November 2026

Manuscript (double-spaced and continuously LINE and PAGE numbered)-for final publication

Click here to view linked References

The Water Footprint of Hydrogen Production

Damola Olaitan[1], Matteo Bertagni[1,2], and Amilcare Porporato[1,2]

[1]Department of Civil and Environmental Engineering, Princeton University, Princeton, NJ, 08540, USA

[2]The High Meadows Environmental Institute, Princeton University, Princeton, NJ, 08540, USA

Corresponding Author: Amilcare Porporato, aporpora@princeton.edu, +1 (609) – 258 – 2287, Engineering Quadrangle, Princeton University, Princeton, NJ, 08540, USA.

Abstract

Hydrogen (H_2) is the most promising energy carrier for reducing the carbon emissions of the energy sector, but the impact of its production on water resources remains unclear. Here, we quantify the water footprint (WF) of different H_2 production pathways accounting for the WF of the primary energy used in the production process, as well as feedstock and infrastructure water requirements. Results suggest that green H_2 obtained from water electrolysis powered by renewable energy has the lowest WF (65±2 m^3/TJ for wind and 204±79 m^3/TJ for solar) mostly due to the low WF of renewable energy. The WF of blue H_2 derived from fossil fuels is significantly higher (369±30 m^3/TJ for natural gas and 564±82 m^3/TJ for coal) due to high WF of fossil fuels as well as the water required for carbon capture and storage (CCS). H_2 produced from nuclear energy and biomass have extremely high WF (741±277 m^3/TJ for nuclear and >50000 m^3/TJ for biomass). Considering global and country-based energy scenarios, where the main H_2 colors (green and blue) individually account for 15% of energy consumption, we find that the use of green H_2 could reduce the water demand of the energy sector while blue H_2 would generally increase it,

except in countries already characterized by high water consumption due to reliance on water-intensive energy sources. At the global level, we find that for every 5% of H_2 energy adoption, the energy sector could have water savings between 1 - 4% for green H_2 and increase water consumption between 1 - 5% for blue H_2. These results highlight the potential and criticalities of H_2 within the water-energy nexus.

Keywords: Water footprint, Hydrogen, Energy Transition

1. Introduction

Hydrogen (H_2) has been receiving a great deal of attention as the low-carbon energy carrier of the future (Hydrogen Council, 2023; IEA, 2022a). The current H_2 demand of 94 Mt in 2021 (IEA, 2022a) is mostly for the refining and fertilizer industries, but new H_2 applications are expected to develop in industry, transport sector, and power generation (IEA, 2022a). Announced pledges to produce new H_2 are rising rapidly and extensively around the world, e.g., from 66 Mt H_2/yr in the 2021 hydrogen projects database to 106 Mt H_2/yr in its 2022 update (IEA, 2022b). Production strategies involve multiple approaches, but particularly via either water electrolysis powered by renewable energy or fossil fuel with Carbon Capture and Storage (CCS), referred to as green and blue H_2, respectively. Other production pathways may include water electrolysis powered by nuclear energy (pink H_2) and H_2 from biomass (brown H_2). The H_2 color scheme utilized in this manuscript follows from the summary by Incer-Valverde et al. (2023).

The global distribution of announced pledges is shown in Figure 1(a), along with the top prospective H_2-producing countries (Fig, 1b). Countries with significant H_2 production pledges have either access to abundant renewable energy necessary to produce green H_2 or a heavy reliance

on fossil fuels, which requires inclusion of low-carbon energy solutions into the energy mix (blue H_2) to meet decarbonization goals.

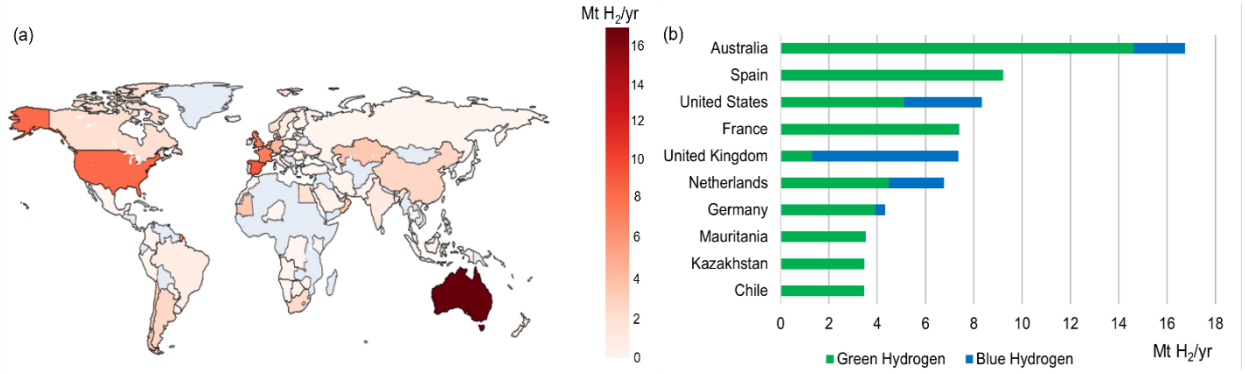


Figure 1. Global pledges for low-carbon H_2 production from data of the International Energy Agency (IEA, 2022b). (a) Global distribution, (b) Top ten prospective H_2 producing countries. Color bar represents the pathway of H_2 production.

The impact of H_2 production on the water-energy nexus remains uncertain, and the intensity of H_2 energy on water resources necessitates thorough quantification for a comprehensive understanding. Consequently, the integration of H_2 into energy transition strategies necessitates an examination of how H_2 impacts the water demand of energy sector at both regional and global scale, bearing in mind the several underlying determinants which can influence these dynamics, including the quantity of H_2 demand, pathway of production, and infrastructural requirements (with or without CCS technologies), amongst others. Previous works (Beswick et al., 2021; Tonelli et al., 2023) quantified the amount of water required globally for a proposed future green H_2 demand and observed that this requirement is small compared to the current amount of water utilized in the fossil fuel sector or in agriculture. Specifically, the geographically explicit analysis (Tonelli et al., 2023) reported that the water required for a global green H_2 demand of 400 MtH_2/yr in 2050 does not create water scarcity almost anywhere in the world if water scarcity is not already

present. However, one the one hand these previous works (Beswick et al., 2021; Tonelli et al., 2023) focused on green H_2 only, while on the other hand, other works on quantifying the water requirements of H_2 production (e.g., Lampert et al. 2015 and Mehmeti et al., 2018) only provided numerical values for the water requirements without a clear analysis of how the reported values are obtained, and neglected the water requirement of the primary raw material or energy source, leaving unclear the total water requirement of different H_2 production methods and how these can impact regional and global resources. Such an analysis is required, especially considering that a high percentage of the water required for energy is locally sourced and the majority of the proposed green H_2 projects are in countries with abundant renewable energy potential but limited water availability.

The water-energy connection of the H_2 economy is already apparent in Figure 2, where we show the country-level H_2 production pledges as a function of physical and economical water scarcities. The physical water scarcity may be quantified by the dryness index (DI), a crucial index in the hydrological sciences (Porporato & Yin, 2022), obtained as a ratio of potential evapotranspiration and precipitation. The dryness index is related to the tendency of a region to be susceptible to water stress or scarcity in the presence of a perturbation in water demand. The Economic Water Scarcity (EWS) is defined as a situation in which technical and institutional capacities or financial resources are insufficient to supply adequate water quantities for human use (Molden, 2013; Rosa et al., 2020; Vallino et al., 2020), and quantified as the complement of the sustainable development goals (SDG) indicator 6.5.1 on the Integrated Water Resources Management (IWRM), i.e., EWS = 1 - IWRM. The indicator assesses water governance and management, providing a framework to determine if water resources are managed equitably, efficiently, and sustainably in each country. EWS is close to one when low level of water

management is present and to zero when best water management is attained (Vallino et al., 2021). The majority of the proposed green H_2 projects are in countries with limited water availability (DI>1), while blue H_2 projects tend to be in water-abundant countries (DI<1). From a socioeconomic perspective, countries with efficient water management strategies (EWS<0.4) account for a larger proportion of H_2 production pledges.

The water-product connection prompted researchers to introduce the concept of Water Footprint (WF), which measures the volume of freshwater used to produce a product (here energy, so that WF is in m^3 of water per TJ of energy produced) over the full supply chain (Egan, 2011).

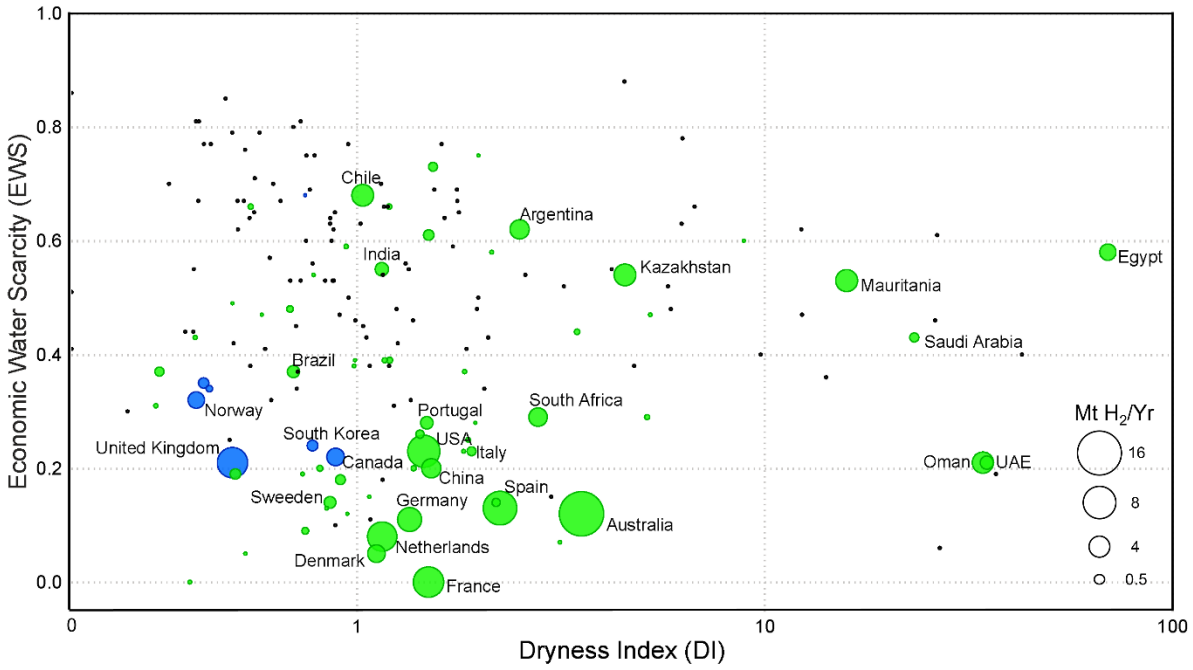


Figure 2. H_2 production pledges as a function of economic water scarcity (EWS) and dryness index (DI). The size of each circle is proportional to the H_2 production pledge (Mt H_2/yr). Dryness index axis in log scale. Black points are countries with no H_2 production pledge, blue points represent countries whose pledged H_2 production is majorly from the fossil fuels pathway, while green points represent countries whose pledged H_2 production is majorly from the water

electrolysis pathway (IEA, 2022b). Data for EWS was obtained from Harris et al. (2020), and DI from UNEP (2021).

The assessment of the WF follows two distinct approaches (Postle et al., 2012; UNEP, 2021; Vanham & Bidoglio, 2013): (1) the volumetric approach which measures the volume of water required for production and (2) the Life Cycle Analysis approach described in (UNEP, 2021) extends beyond production and evaluates the environmental performance of products and services along their life cycle. This paper estimates the WF of H_2 production using the volumetric approach (Hoekstra et al., 2012) and accordingly, the WF of H_2 provides information about the total volume of water required for production, and this quantity can be influenced by several underlying factors, including the WF of the primary energy sources or raw material required for production, water required for feedstock, as well as the infrastructural water requirements (plant cooling and for CCS facilities in case of energy sources relying on fossil fuels). The WF of a product has three components: (1) blue water which measures the volume of surface or groundwater consumed, (2) green water which measures the volume of rainwater consumed, and (3) grey water which is an indicator of freshwater pollution. In the context of H_2 production, the WF is blue water, except for H_2 produced from biomass (Here, WF would be the sum of green and blue water) which can potentially be rainfed.

Several prior research studies have implemented the concept of WF in the energy sector, displaying varying extents of application and exploration (Barker, 2007; DoE, 2006; Fthenakis & Kim, 2010; Gleick, 1994; Macknick et al., 2011; Mekonnen & Hoekstra, 2011, 2012; Meldrum et al., 2013; Mielke et al., 2010; Mulder et al., 2010; Tuninetti et al., 2015; Wu et al., 2009). Mekonnen et al. (2015) compared the WF of different energy sources and observed that electricity from renewable sources has the smallest WF when compared to fossil fuels, biomass, and

hydropower. Their findings further indicated that operations and fuel supply contribute the most to the WF, while that of plant construction is negligible. More recently, Rosa et al. (2021) found that the WF of CCS technologies can be large, although highly variable (0.74 to 575 m^3per tonne CO_2).

This study endeavors to (1) investigate the WF of H_2 production via different pathways and compare this WF with respect to other energy sources, (2) investigate the effect of H_2 WF on the WF of energy on both regional and global scales. To achieve the first point, we follow the commonly used approach of estimating the WF of a product by considering all streams of water withdrawal (and consumption) for different H_2 production pathways as described in section 2.1-2.3. Consequently, we present in section 2.4 the process of analyzing H_2 WF impact on the energy sector. Such an analysis provides insights into identifying the potential implications H_2 energy might have on water availability and can help decision makers on environmental and energy transition strategies.

2. Methods

To quantify the WF of H_2, we consider the amount of water consumed and polluted in the different stages of the supply chain, depending on the H_2 production pathway. The method utilized in this study to estimate the WF of H_2 follows from the commonly presented approach of estimating the WF of energy (e.g., Mekonnen et al. 2015, Meldrum et.al 2013). Here, we segregate the water requirement for H_2 production into two distinct categories: WF of the primary energy source or raw material and the water requirement for operation, where the later can be subdivided into feedstock water requirement, plant cooling water requirement and additional water required for CCS facilities for energy sources relying on fossil fuels or have substantial carbon emissions.

A general illustration of the steps involved in calculating the WF of H_2 is presented schematically in Figure A1.

We consider the three main pathways for H_2 production, namely water electrolysis, fossil fuel, and biomass. We quantify the WF of H_2 both per unit mass (WFM_{H_2} in m^3 of water/tonne H_2 or kg H_2O/kg H_2) and per unit of energy (WFE_{H_2} in m^3/TJ). The conversion is done through H_2 higher heating value (HHV=0.142 TJ/tonne H_2). The advantage of having the two quantities is that the WFM provides a very intuitive measurement between water and hydrogen masses, while WFE provides a way to compare the water footprint of H_2 energy with other energy sources. The water requirements for operation via the water electrolysis and fossil fuel pathways considered are from the National Renewable Energy Laboratory (NREL), while that of H_2 from biomass is from Binder et al. (2018) converted and expressed here as m^3/tonne .

2.1. Water Electrolysis pathway

This process produces H_2 through the electrochemical conversion of water to H_2 and oxygen ($2H_2O \rightarrow 2H_2 + O_2$). To evaluate the WF of H_2 from water electrolysis, we require the WF of the electricity source (WF_{EL}), the amount of electricity, EL (TJ/tonne H_2), as well as the stoichiometric amount of water as feedstock, *W* (m^3/tonne H_2). The WF of the primary energy is estimated as the product of EL and WF_{EL}, while the water requirement for operation is basically *W*. Hence, WF for this pathway can be calculated as

$$WFM_{H_2} = EL * WF_{EL} + W. \quad (1)$$

We consider electricity from three sources: solar, wind, and nuclear energy. The corresponding values for WF_{EL} (m^3/TJ) are from Mekonnen et al. (2015), see Table T1.

2.2. Fossil Fuel pathway

H_2 is produced from fossil fuel either from natural gas, through steam methane reforming (SMR), or from coal gasification (CG). SMR is currently the most mature production and widely used process for the generation of H_2 in large central plants (IEA, 2022a). By applying high pressure steam to methane, carbon monoxide and syngas (containing H_2) is produced ($CH_4 + 2H_2O \rightarrow CO_2 + 4H_2$). CG technology produces H_2 by reacting coal with oxygen and steam under high pressures and temperatures to produce carbon monoxide and H_2 ($2C + 2H_2O + O_2 \rightarrow 2CO_2 + 2H_2$) (Mehmeti et al., 2018). To determine the WF of H_2 from fossil fuels, we require the amount of fuel, *F* (tonne *F*/ tonne H_2) and the WF per unit mass of fuel, WF_F (m^3/ tonne *F*). In the production process, water is required as feedstock and to cool the plants, *W* (m^3/ tonne H_2), and if carbon capture and storage facilities are put in place, additional water is required, W_{CCS} (m^3/ tonne H_2). The WF of the raw material is estimated as the product of *F* and WF_F, while the water requirement for operation is the sum of *W* and W_{CCS}. As a result, WF for this pathway can be calculated as

$$WFM_{H_2} = F * WF_F + W + W_{CCS}. \quad (2)$$

2.3. Biomass gasification pathway

Biomass and bio-derived fuels can be used to produce H_2 from thermo-chemical and biological routes (Kırtay, 2011). Biomass gasification is a promising pathway for the conversion of biomass into energy products taking place at elevated temperatures, between 500 and 1400 °C without combustion (Iribarren et al., 2014), and it is mostly described as a process with negative GHG emissions attributed to the amount of CO_2 removed from the atmosphere while growing biomass (Salkuyeh et al., 2018; Susmozas et al., 2016). To determine the WF of H_2 from biomass (wood chips), we require the amount of biomass, *B* (tonne *B*/ tonne H_2), the WF per unit mass of the biomass, WF_B (m^3/tonne *B*). Additionally, biodiesel fuel, *F* is used in the scrubber unit to

separate the condensable tar from the product gas (Binder et al., 2018). Water is required as steam to cool the plants, *W*, and if carbon capture and storage facilities are put in place, additional water is required, W_{CCS}. The WF of the raw material is estimated as the sum of the products of *F* and WF_F, and *B* and WF_B while the water requirement for operation is the sum of *W* and W_{CCS}. Hence, WF for this pathway can be calculated as

$$WFM_{H_2} = F * WF_F + B * WF_B + W + W_{CCS} \quad (3)$$

where WF_F of biodiesel (rapeseed methyl ester) is 790 m^3/ tonne biodiesel (Spang et al., 2014). Due to lack of specific references that explicitly provide information about the amount of water required due to CCS facilities, the average of W_{CCS} for coal and natural gas is assumed, as the precise value is liable to be irrelevant since the WF of wood chips is about an order of magnitude higher.

2.4. Energy replacement with H_2

The WF of H_2 per unit energy (m^3/TJ) obtained from different pathways are then used to investigate the impact of partial replacement of H_2 on the water footprint of the energy sector on country and global scales, we use primary energy consumption data from Ritchie et al. (2022) which contains the total amount of energy consumed on a country, region and global scale. Primary energy in this context includes energy that the end user needs, in the form of electricity, transport and heating, plus inefficiencies and energy that is lost when raw resources are transformed into a usable form. Globally, net-zero energy scenarios are considering H_2 to potentially account for up to 15% (Gielen et al., 2019; IEA, 2021) of the final energy consumption, where a certain quota must have been lost due to energy conversion inefficiencies. To this end, we assumed a 15% partial energy replacement with H_2 distinctively considering blue and green H_2 on the country

scale, while on a global scale, we considered a replacement of 0 - 25% at a 5% increase to illustrate the effects of a gradual global energy transition scheme.

3. Results

3.1 Comparison with other energy sources

The WF of producing H_2 via different pathways (bars are color coded following Incer-Valverde et al. (2023) with respect to the hydrogen production pathway) is presented in Figure 3 in comparison with other energy sources. The numerical results are also reported in Table 1. The WF of firewood, nuclear, oil, coal and lignite, geothermal, natural gas, solar and wind energy are obtained from Mekonnen et al. (2015), converted and represented here as WF per energy unit rather than WF for electricity, as presented in the referenced paper. Provided that variation exists in plant cooling techniques, CCS technologies, as well as method of extraction of raw materials, we also utilized the maximum and minimum values reported in Mekonnen et al. (2015) to evaluate an upper and lower bound for the WF of H_2.

The WF of H_2 is lowest when it is produced from the water electrolysis pathway, particularly when electricity is provided by renewable sources, such as wind and solar energy. Green H_2 from solar (204±79 m^3/TJ) exhibits a similar WF compared to conventional fossil fuels, with potential for a reduced WF through advancements in electrolyzer and electrification efficiency. Green H_2 from wind (65±2 m^3/TJ) has a significantly lower WF. Conversely, when electricity is sourced from nuclear energy (pink H_2), the WF is higher (741±277 m^3/TJ), mostly due to the high WF of nuclear energy. Blue H_2 produced from natural gas (369±30 m^3/TJ), and coal (564±82 m^3/TJ) demonstrates a much higher WF compared to green H_2 obtained from water electrolysis. The highest WF is for brown H_2 derived from biomass (>50000 m^3/TJ), primarily attributed to the significant WF associated with wood chips and biodiesel. With regards to the WF

of blue H_2, the analysis by D'Odorico et al. (2017) suggests that the WF of fossil fuels (coal, oil and natural gas) are usually underestimated since they do not account for consumption of embodied (ancient) water from the geologic past. With such a consideration, it can be assumed that the WF of H_2 form fossil fuels presented here is tentatively underestimated. A linear scale of the WF of H_2 from different pathways is presented in Figure 3(b) to elucidate the difference between the WF of green and blue H_2.

Amongst the components considered to estimate the WF of H_2, the WF of the energy source contributes the most to the total WF (Table 1), except for wind energy, attributable to its low WF of electricity (1.2-12 m^3/TJ). The amount of water required during the production process of blue H_2 is larger than the amount that could have been calculated directly from the stoichiometric analysis of the chemical reaction, as additional water is required for cooling and to drive the production process (Lampert et al., 2015). Penev (2022a, 2022b) reports the amount of water required for SMR with and without the consideration of CCS technologies respectively, while Penev (2022c) and Rutkowski & Darlene (2008) reports the amount of water required for CG with and without the consideration of CCS technologies respectively. The sum of water required for feedstock, steam and CCS facilities is similar in both fossil fuel pathways with values of 30.2 m^3/ tonne H_2, and 29.5 m^3/ tonne H_2 for natural gas and coal respectively. However, the disparity in the total WF is attributed to the WF and *F* specific to each fuel source, with values of *F* for natural gas (3.2 tonne CH_4/ tonne H_2), and coal (8.73 tonne C/ tonne H_2). Advances to this method of estimating the WF of H_2 casually stems from better documentation of process water flow, and the advent of new production methods, e.g., Guo et al. (2022) presents a how H_2 can be produced from the direct capture of water vapor from air which eliminates several components of equations 1-3. Osselin et al. (2022) presents a technique through which water is injected in situ in identified

256 reactive formations and H_2 saturated water (termed as orange H_2) is collected from recovery wells
257 surrounding the injection point. Although these methods are yet to be implemented globally on a
258 large scale.

Table 1. Components to estimate WF of H_2 per unit mass (WFM) and unit energy (WFE). The conversion is based on the high heating value of H_2 (0.142 TJ/ tonne H_2).

Pathway	Primary energy source	Energy WF (m^3/ tonne H_2)	W (m^3/ tonne H_2)	W_{CCS} (m^3/ tonne H_2)	WFM_{H_2} (m^3/ tonne H_2)	WFE_{H_2} (m^3/TJ)
Water Electrolysis[a]	Solar	20	9	0	29	204
	Wind	0.2	9	0	9.2	65
	Nuclear	96	9	0	105	741
Fossil fuel	Coal (CG)[b]	50	16[e]	13.5	80	564
	Natural gas (SMR)[c]	22	16[f]	14.2	52.4	369
Biomass	Wood chips[d]	7450	3.4	13.8[*]	7467	52586

Sources: a) DeSantis et al. (2020), b) Penev (2022c), c)Penev (2022a), d) Binder et al. (2018), e) Rutkowski & Darlene (2008) , f) Penev (2022b).

[*]W_{CCS} of biomass gasification is assumed to be an average of W_{CCS} for coal and natural gas, due to lack of specific references that explicitly provide information about the amount of water due to CCS facilities.

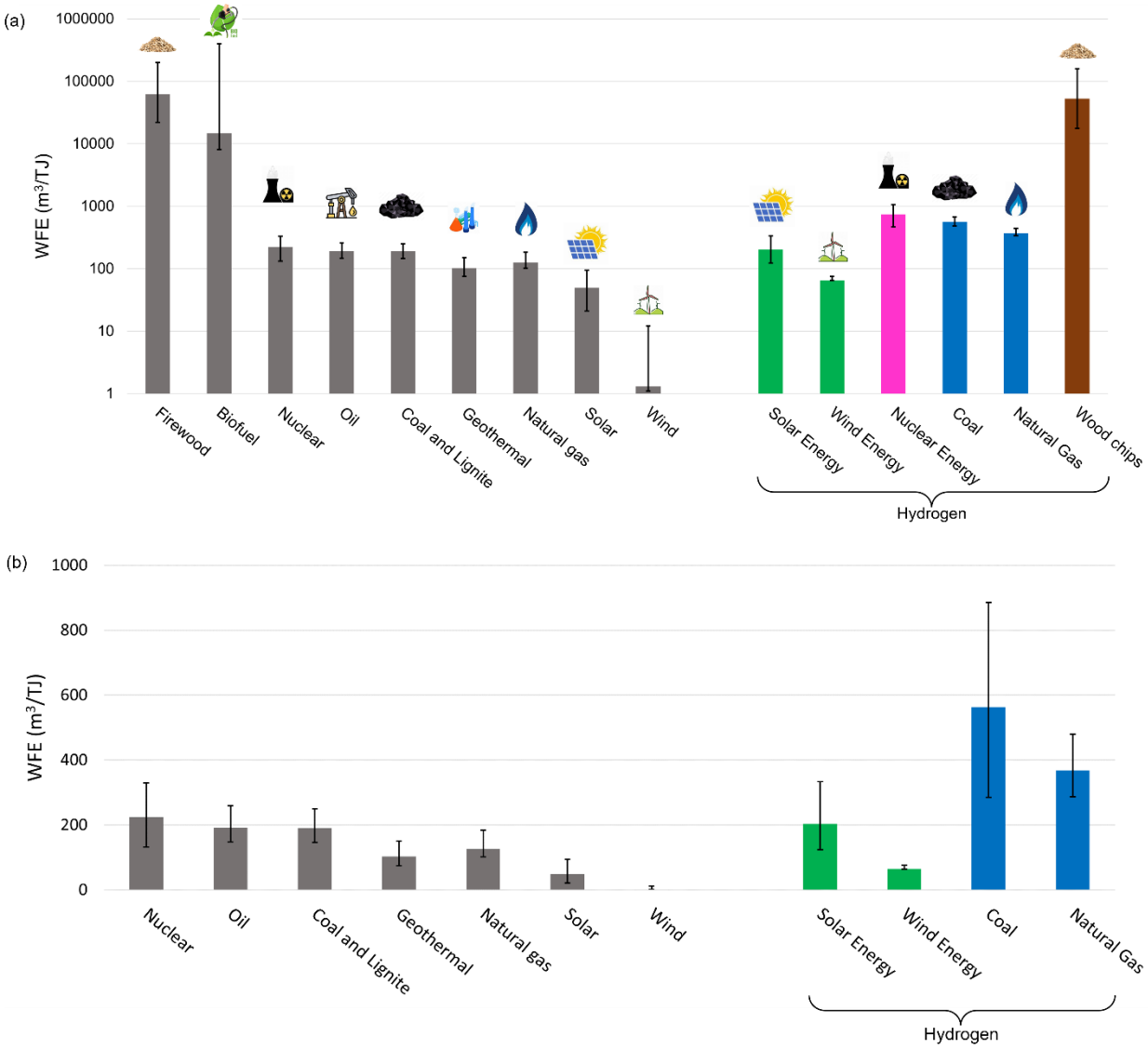


Figure 3. Average water footprint per unit energy (WFE) of H_2 and other energy sources. The ranges reflect the maximum and minimum values for each energy source. For H_2, range of values is obtained by utilizing the upper and lower bound the WF of individual energy sources as presented by Mekonnen et al. (2015). The y-axis is (a) in log scale, while that of (b) in linear scale to juxtapose the difference between the WF of green H_2 and blue H_2.

3.2 H_2 impact on the water footprint of the energy sector.

3.2.1. Country-scale scenarios.

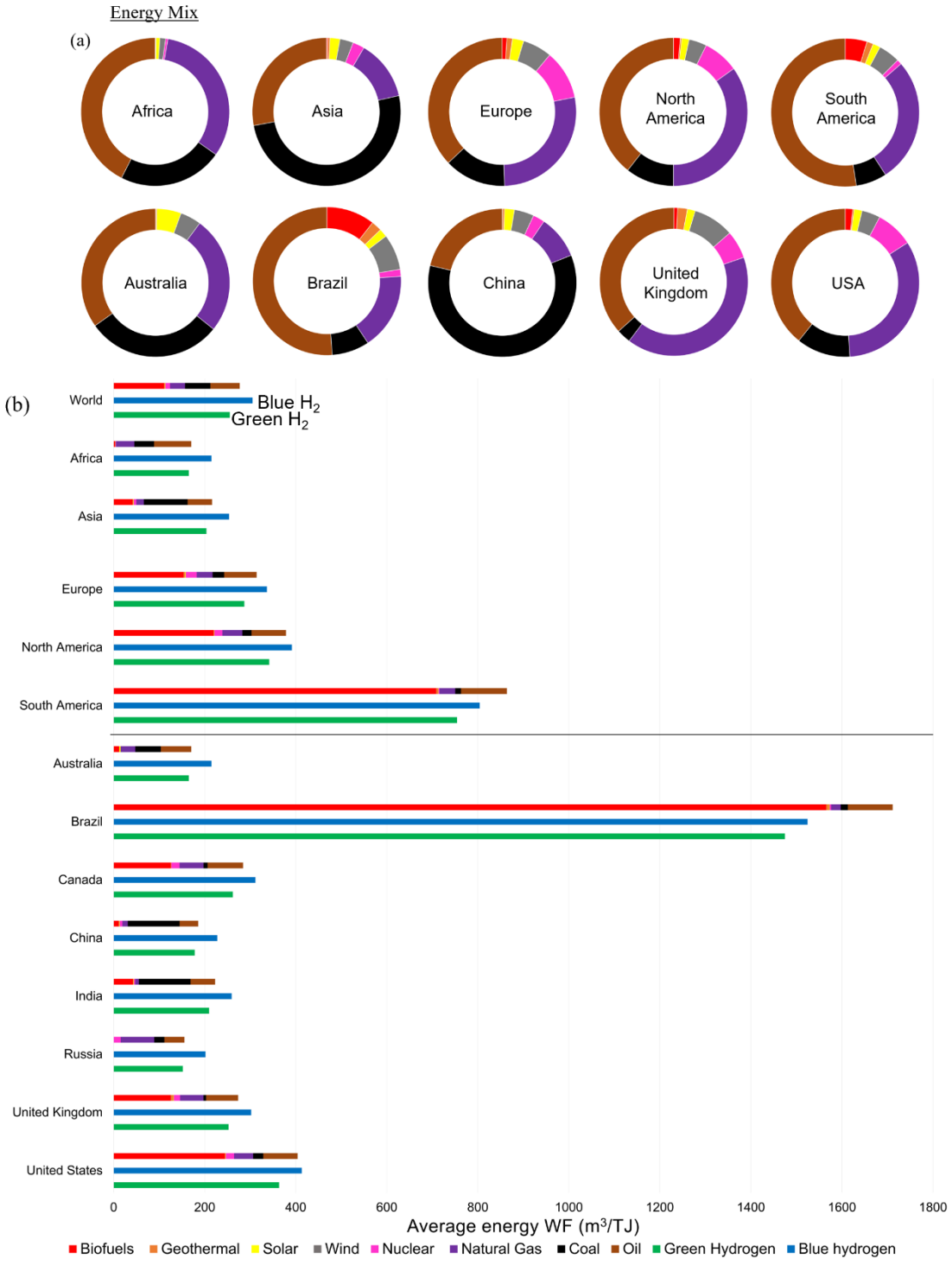
In this section, we estimate the water footprint associated with partial energy replacement scenarios distinctively involving the main hydrogen colors namely, green and blue H_2. The water demand of each country energy is estimated as the sum of the products of primary energy consumption data delineated by source (Ritchie et al., 2022) and the corresponding energy WF. The energy mix of selected countries and regions is reported in Figure 4(a), showing the contribution of individual energy sources to the total energy consumed. The average WF of each country energy mix is estimated as the ratio of the total water demand to the total energy consumed. The country WF mix is presented in every first bar in Figure 4(b). We have neglected the contribution of hydropower to the total energy consumed, following previous studies (e.g., Macknick et al., 2012; Spang et al., 2014), based on the fact that reservoirs are generally multi-purpose, therefore making it challenging to accurately estimate the amount of evapotranspiration water loss (WF of hydropower), solely to hydroelectric power generation. Typically, some studies allocate a certain percentage of the total water evaporated from a reservoir based on the purpose of the reservoir, however, this allocation is considered ambiguous (Macknick et al., 2012; Spang et al., 2014).

To estimate H_2 impact on the energy consumed, we consider a scenario whereby 15% of the primary energy consumed is met by H_2 (green and blue separately). The individual green and blue bars in Figure 4(b) represent what would have been the WF of these selected countries and regions if 15% of the primary energy consumed was provided by green or blue H_2. Our result suggests that green H_2 has potential of reducing the WF while blue H_2 causes an increase in WF except for Brazil and the South American region, attributable to their originally high WF.

The influence of green H_2 is perceived to be beneficial, most especially in regions with initially high WF, while its influence was minimal in regions with initially lower WF. Regional primary energy consumption and its energy mix play a critical role in reducing the WF when replacing conventional fuel with green H_2. For instance, Africa's low primary energy consumption coupled with a low current WF diminishes the impact of green H_2 as a replacement fuel. Conversely, regions with high primary energy consumption often exhibit elevated WFs, highlighting the significance of green H_2 in such contexts.

A suggested replacement strategy would be to reduce the reliance on water-intensive energy sources, given that they exert a significant impact on the WF even when consumed in minute proportions. For instance, despite accounting for less than 2%, 1%, and 1% in the USA, Canada, and the United Kingdom respectively, biofuel has the highest (60%, 44%, and 45% for USA, Canada, and the United Kingdom respectively) contribution to these regions WF.

A high WF of the energy sector may have very different impacts depending on the local availability of water resources. In water-limited regions, water demand for energy can pose threats to the sustainability of other water users (agriculture, industry etc.). Our estimates of H_2 WF are under the assumption that all water components of equations 1-3 are locally sourced. Relaxing this assumption would require exploring the trade of raw materials (natural gas, coal, and biomass) and the associated virtual water trade (A. Y. Hoekstra & Hung, 2003) can affect the WF of H_2. Under such conditions, the solely locally sourced components of the WF (equation 2) during production will be limited to water requirements for operation (W and W_{ccs}).



315

316 **Figure 4.** (a) Energy mix of selected countries and regions showing the relative contribution of

317 individual energy sources in the total energy consumption. Energy data are from Ritchie et al.

(2022) for the year 2021. (b) Average water footprint of energy (m^3/TJ). For each country or region, the first bar and labels are presented to indicate individual energy sources, while full green and blue bars represent a scenario of where green and blue H_2 account for 15% of the energy mix, respectively.

3.2.2. Global scenarios

Energy transition scenarios allocate a specific share for H_2 within the overall energy mix. For example, the International Renewable Energy Agency (IRENA) projects up to 19 EJ (~6% of total final energy consumption – 351 EJ) of energy for electrification provided by H_2 (Gielen et al., 2019). In the Net Zero Emissions (NZE) by 2050 report published by the IEA (IEA , 2021), hydrogen-based fuels are projected to provide up to 33 EJ (~10%) of the total final energy consumption.

H_2 energy is believed to enhance energy security through a decreased dependence on fossil fuels, and a diversified energy mix (IEA, 2022b). Here, we investigate the effect of a 5 - 25% partial energy replacement on the global WF associated with primary energy consumption. For the global scenarios, we consider the main H_2 colors, namely green and blue, since other pathways like biomass and nuclear energy have negligible consideration in the announced production pledges (IEA, 2022b). Reported in Figure 5 is the percentage difference in the global WF as a result of H_2 partial energy replacement. For every 5% H_2 partial energy replacement, we observe a 4% reduction in the global WF when water electrolysis and wind energy is the production source, while for solar energy, the percentage reduction was 1.3%. The effect was opposite when the H_2 production was from fossil fuel, with a 1.6% increase in WF when the source was natural gas, and 5.2% from coal. These results promote renewable energy usage, particularly solar and wind energy, coupled with the electrification of the energy sector.

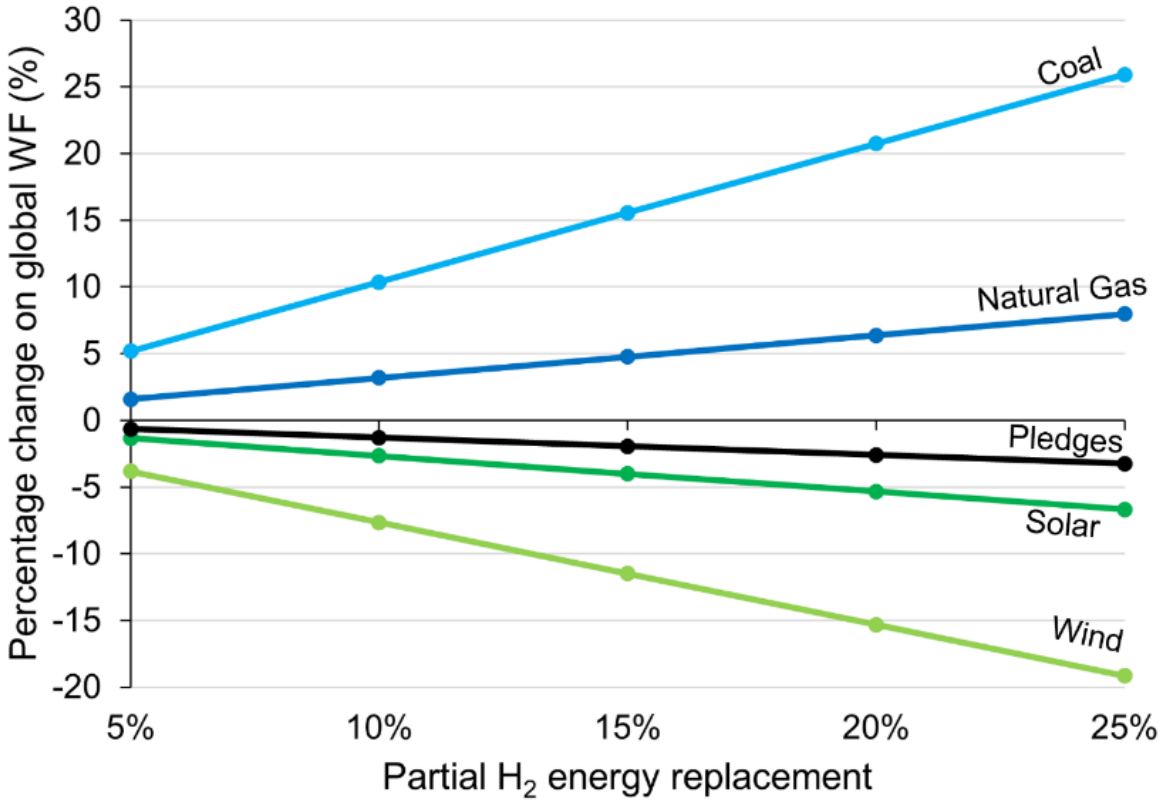


Figure 5. Effect of partial energy replacement with H_2 energy on the global WF of energy. Labels show the source from which H_2 is produced.

To achieve a reduced global WF of energy upon introduction of H_2 into the energy mix, Figure 5 suggests that such H_2 must be produced by water electrolysis, with energy sources of wind, solar, or a combination of both. A small portion of the global H_2 demand can be met by blue H_2 while still achieving the goal of reduced WF. This is illustrated by the black line in Figure 5 which represents a blend of green (80%) and blue (20%) H_2, aligning with the announced pledges for H_2 production. The results show a 0.7% reduction in global WF for every 5% H_2 partial energy replacement. Hence, upon the fulfillment of the announced pledges, a decrease in WF of the energy sector is anticipated, along with numerous other advantages associated with the integration of H_2 into the energy mix.

4. Discussion

The H_2 economy has been experiencing significant growth in recent years, driven by a commitment to adopt low-carbon energy sources with the overarching goal of achieving net-zero emissions, leading to a question about the water requirements of H_2 production which has been lingering in recent years (Beswick et al., 2021; Lampert et al., 2015; Mehmeti et al., 2018; Tonelli et al., 2023). This fundamental question is one of the bases of discussion when new energy sources are planned to be utilized on large-scale, alongside other questions such as energy sustainability and security, storage, among others. Here, we have presented the water implications of producing H_2 and implementing it into energy transition scenarios and results, such as the capacity of green H_2 to reduce water demand of the energy sector, corroborate existing evidence of H_2 playing a vital role in satisfying future energy demands.

The WF of H_2 carries a large variability due to diverse production pathways and the result suggests that green H_2 has a lower WF compared to blue H_2 while H_2 from nuclear energy and biomass have much higher WF. Our finding on green H_2 is remarkably similar to Tonelli et al.'s observation on how green H_2 powered by wind energy has a smaller water requirement compared to green H_2 powered by solar energy. Considering that both pathways have the same stoichiometric water requirements, this striking contrast is as a result of wind energy having a much smaller WF than solar energy (Mekonnen et al., 2015; Meldrum et al., 2013; Spang et al., 2014). The high WF of nuclear energy is also why H_2 possesses a high WF when it is the source of power for water electrolysis. Our findings that blue H_2 from SMR has a lower water requirement than that from CG correlates with Mehmeti et al.'s observation, although the reported numbers are remarkably different.

Implementing H_2 into the energy mix of a country can either increase or decrease their water demand for energy depending on the H_2 production pathway, the amount of H_2 demand, and the available resources. The influence on water resources is tentatively different on varying spatial and temporal scales, as on smaller scales, the production of H_2 can lead to local water scarcity, without a substantial effect on country scale water consumption. This calls for location optimization analysis (e.g., for solar and wind energy, Azadeh et al., 2008, 2011; Ruiz et al., 2020; Zoghi et al., 2017) to accurately determine suitable locations for H_2 production plants, taking into account all underlying limitations during the production process.

It is typical that countries will consume a combination of green and blue H_2 as the required resources vary in abundance in every region. A proper consideration of local water competition should be a crucial factor in determining H_2 production sites to avoid exacerbating local water competition. For instance, investigating a scenario of water demand for H_2 production to fuel electric vehicles, Lee et al. (2019) found that, while the amount of water consumed in California would be only 1.3 times that consumed in New York state, resulting water scarcity footprint would be 27 times higher due to the low water availability in California. According to our Figure 2, several countries characterized with elevated levels of physical water scarcity (DI>10), including Egypt, UAE, Oman, Saudi Arabia, and Mauritania have committed to H_2 production. This indicates that physical water limitations may be a local-to-regional problem, given the lack of abundant water resources and competition with other water users.

In addition to physical water scarcity, some countries with H_2 production pledges (e.g., Egypt, Kazakhstan, and Mauritania) exhibit economic water scarcity (EWS > 0.5, Figure 2). In order for the proposed H_2 production to not exacerbate a lack of water resources, it will be crucial for these countries to implement efficient water management. Conversely, countries such as

France, Netherlands, Germany, Spain, Australia, USA with an EWS < 0.25, are primarily tasked with situating production sites in areas where local water scarcity will not be exacerbated to fulfill their pledged production targets.

It is also important to examine green and blue H_2 from a holistic environmental lens. The use of green H_2 clearly reduces the reliance on fossil fuels consumption and promotes the use of renewable energy. By contrast, the use of blue H_2 relies on an increased extraction and use of fossil fuels (due to the energy penalty in the fossil fuel to H_2 conversion). This would have several environmental consequences, including a potential increase in fugitive emissions of methane (Bertagni et al., 2022; Howarth & Jacobson, 2021). Moreover, due to inefficiency in CCS processes (e.g., 60-90% CO_2 capture rate, Brandl et al., 2021 and references therein), blue H_2 would still entail some CO_2 emissions. Following research on energy sustainability, we find that the best way to mitigate carbon emissions and reduce water consumption through H_2 production is to promote the use of renewable energy other than considering alternative emissions reduction techniques, such as CCS technologies (D'Odorico et al., 2017; Rosa et al., 2021). Therefore, the supremacy of green H_2 over other production pathways extends beyond just having a smaller WF, but also to economic and environmental sustainability. As an additional remark, for any H_2 color and production pathway, it will be crucial to reduce H_2 fugitive emissions due to H_2 indirect greenhouse gas effect (Paulot et al., 2021; Sand et al., 2023).

While it is not immediate that the distinction in the water source for green H_2 (freshwater) and blue H_2 (fresh- or saltwater) is significant factor in their comparative assessment, an analysis by Beswick et al. (2021) demonstrates that desalination of salt water presents a viable alternative, although this added process will cause an increase in energy demand and economic cost of producing green H_2. It is essential to acknowledge that recent research are also considering the

production of green H_2 from treated wastewater (Jack et al., 2021; Jiang et al., 2023; Rousseau et al., 2020). Blue H_2 is currently less expensive than green H_2 with prices ranges of 1.4 – 3.2 US $ /kg H_2 and 1.9 – 8.2 US $ /kg H_2 for blue and green H_2 respectively (IEA, 2019, 2022a; Togni & Fakoury, 2022; UNECE, 2021). Blue H_2 has lower prices as it's the current widely used production technology, but their prices are hypothesized to increase upon the consideration of CO_2 taxes, plummet in the reliance of fossil fuels or due to energy crises, while the actuation of the announced pledges to produce green H_2, growth of renewable energy consumption and improvement of energy convergence efficiency for solar and wind energy will tentatively lead to reduced prices for green H_2.

5. Conclusions

We investigated the potential impacts that hydrogen (H_2) energy may have on water resources following the interests of governments and organizations to incorporate H_2 into the energy mix. For the main production pathways, we considered the WF of energy sources, the water required for feedstock or steam, and WF of CCS technologies. Overall, H_2 has a relatively high WF compared to other energy forms but with a great variability depending on the H_2 production pathway. H_2 production through water electrolysis, particularly when powered by renewable sources such as solar and wind energy, results in the lowest WF. Conversely, H_2 produced from biomass exhibits the largest water footprint, primarily due to the high WF associated with biomass production. There remains the possibility of a reduced WF associated with green H_2 production as advancements in electrolyzer efficiency continue to unfold in the future.

Given the influence of the energy mix on the WF of a region, it is essential to consider a transition from water-intensive energy sources to achieve reduced water demand by the energy sector, especially in regions with minimal water resource availability. Our results (Figure 4 and 5)

highlight the water-saving capabilities of green H_2 derived from wind energy. This approach not only offers water-saving benefits but also contributes to the overall advantages of utilizing low-carbon energy sources, and this corroborates the announced production pledges (IEA, 2022b), as 81% of total H_2 pledges are to be produced from the water electrolysis pathway with renewable energy. The utilization of fossil fuel based H_2 production with CCS would instead exacerbate the anthropogenic pressure on water resources and should hence be considered justifiable only in regions endowed with abundant fossil fuel resources, CCS facilities, and water resources.

Improved data availability in the future will allow further exploration of the H_2 impacts on the water-energy nexus and a detailed knowledge of water requirements for hydrogen production will add useful information (e.g., source of water green, blue, grey) to enable improved attribution of H_2 WF, necessitate a LCA analysis, and determine sustainable proportioning of green and blue H_2 into their energy mix.

Appendix

The water footprint for electricity (WF_{EL}) required for equation 1 is obtained from (Mekonnen et al., 2015), with values reported in Table T1, and for this work, we have only considered electricity from solar, wind and nuclear energy. Simultaneously, to convert the average consumptive WF per unit electricity and heat produced obtained from (Mekonnen et al., 2015), the energy conversion efficiency is required and presented in Table T2 for individual energy source.

Figure A1 on the other hand represents a schematic approach to the estimation of the WF of H_2 from the three considered pathways, displaying the water requirements of each process.

Table T1. Average consumptive WF per unit of electricity and heat produced (Mekonnen et al., 2015).

Energy source	WF (m^3/TJ_e)
Firewood	156400
Nuclear	678.3
Oil	496.1
Coal and Lignite	495.1
Geothermal	342.1
Natural gas	247.1
Solar	140
Wind	1.3

Table T2. Energy Conversion Efficiency

Energy Source	Efficiency (%)	References
Coal	38	Meldrum et al. (2013)
Oil	39	Meldrum et al. (2013)
Natural gas	51	IEA (2000)
Nuclear	33	Meldrum et al. (2013)
Biomass	20 - 40	Faaij (2006)
Geothermal	12 - 25	Zarrouk & Moon (2014)
Solar	20 – 35	Crabtree & Lewis (2007)
Wind	20 – 40	EPA (2013)
Hydropower	85 - 90	Power (2005)

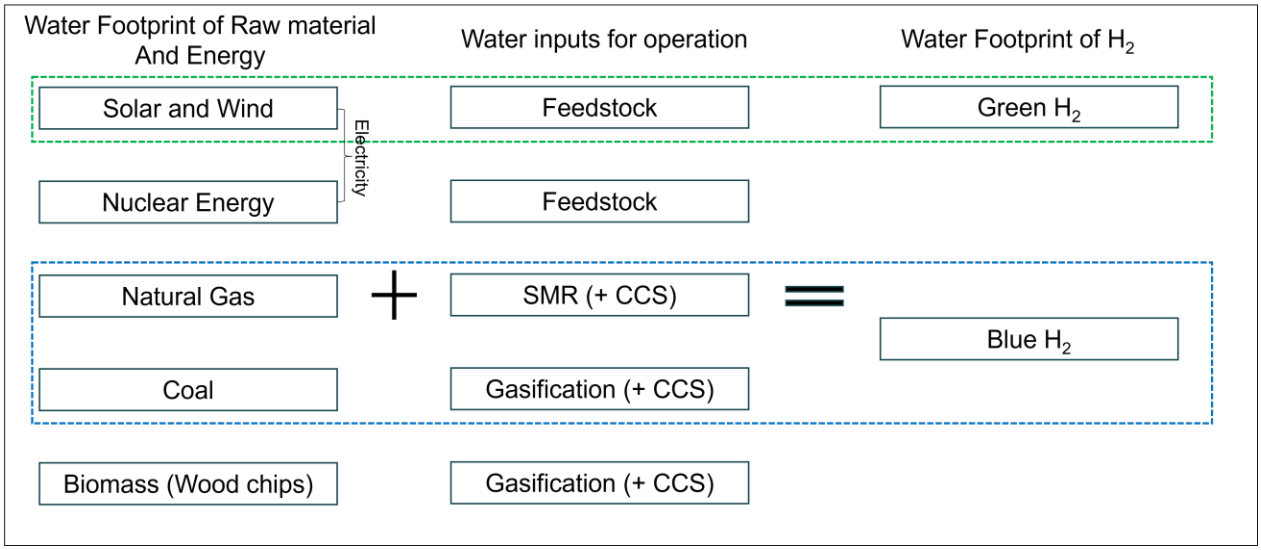


Figure A1. Schematic representation of the WF of H_2 production process.

CRediT authorship contribution statement

All authors have significantly contributed to the success of this research from the conceptualization phase to the first draft of the manuscript. **Damola Olaitan**: Conceptualization, Data curation, Formal analysis, Investigation, Visualization, Writing – original draft. **Matteo Bertagni**: Conceptualization, Investigation, Methodology, Writing – review & editing. **Amilcare Porporato**: Conceptualization , Investigation, Writing – review & editing, Supervision, Funding acquisition.

Declaration of competing interest

All authors state that they have nothing to declare.

Data availability

Datasets for this research are available in Harris et al. (2020), IEA (2022), Ritchie et al. (2022), and UNEP (2021).

Acknowledgements

M.B.B. was supported by the BP Carbon Mitigation Initiative (CMI) at Princeton University. A.P. acknowledges the support from the BP through the CMI at Princeton University.

References

Azadeh, A., Ghaderi, S. F., & Nasrollahi, M. R. (2011). Location optimization of wind plants in Iran by an integrated hierarchical Data Envelopment Analysis. *Renewable Energy*, *36*(5), 1621–1631. https://doi.org/10.1016/j.renene.2010.11.004

Azadeh, A., Ghaderi, S., & Maghsoudi, A. (2008). Location optimization of solar plants by an integrated hierarchical DEA PCA approach. *Energy Policy*, *36*(10), 3993–4004.

Barker, B. (2007). Running dry at the power plant. *Epri Journal*.

Bertagni, M. B., Pacala, S. W., Paulot, F., & Porporato, A. (2022). Risk of the hydrogen economy for atmospheric methane. *Nature Communications*, *13*(1), 7706. https://doi.org/10.1038/s41467-022-35419-7

Beswick, R. R., Oliveira, A. M., & Yan, Y. (2021). Does the Green Hydrogen Economy Have a Water Problem? *ACS Energy Letters*, *6*(9), 3167–3169. https://doi.org/10.1021/acsenergylett.1c01375

Binder, M., Kraussler, M., Kuba, M., & Luisser, M. (2018). Hydrogen from Biomass Gasification—IEA Bioenergy. *IEA: Paris, France*.

Brandl, P., Bui, M., Hallett, J. P., & Mac Dowell, N. (2021). Beyond 90% capture: Possible, but at what cost? *International Journal of Greenhouse Gas Control*, *105*, 103239. https://doi.org/10.1016/j.ijggc.2020.103239

Crabtree, G. W., & Lewis, N. S. (2007). Solar energy conversion. *Physics Today*, *60*(3), 37–42.

DeSantis, D., James, B., & Saur, G. (2020). Hydrogen Analysis Production Models. *Solid Oxide Electrolysis Case (Current)*. https://www.nrel.gov/hydrogen/assets/docs/current-central-solid-oxide-electrolysis-version-nov20.xlsm

D'Odorico, P., Natyzak, J. L., Castner, E. A., Davis, K. F., Emery, K. A., Gephart, J. A., Leach, A. M., Pace, M. L., & Galloway, J. N. (2017). Ancient water supports today's energy needs. *Earth's Future*, *5*(5), 515–519.

DoE, U. (2006). Energy demands on water resources: Report to Congress on the interdependency of energy and water. *Washington DC: US Department of Energy*, *1*.

Egan, M. (2011). The Water Footprint Assessment Manual. Setting the Global Standard. *Social and Environmental Accountability Journal*, *31*(2), 181–182. https://doi.org/10.1080/0969160X.2011.593864

EPA. (2013). *Renewable Energy Fact Sheet: Wind Turbines*. United States, Environmental Protection Agency. https://www.epa.gov/sites/default/files/2019-08/documents/wind_turbines_fact_sheet_p100il8k.pdf

Faaij, A. (2006). Modern biomass conversion technologies. *Mitigation and Adaptation Strategies for Global Change*, *11*, 343–375.

Fthenakis, V., & Kim, H. C. (2010). Life-cycle uses of water in US electricity generation. *Renewable and Sustainable Energy Reviews*, *14*(7), 2039–2048.

Gielen, D., Gorini, R., Wagner, N., Leme, R., Gutierrez, L., Prakash, G., Asmelash, E., Janeiro, L., Gallina, G., & Vale, G. (2019). Global energy transformation: A roadmap to 2050. *Hydrogen Knowledge Centre*.

Gleick, P. H. (1994). Water and Energy. *Annual Review of Energy and the Environment*, *19*(1), 267–299. https://doi.org/10.1146/annurev.eg.19.110194.001411

Guo, J., Zhang, Y., Zavabeti, A., Chen, K., Guo, Y., Hu, G., Fan, X., & Li, G. K. (2022). Hydrogen production from the air. *Nature Communications*, *13*(1), 5046. https://doi.org/10.1038/s41467-022-32652-y

Harris, I., Osborn, T. J., Jones, P., & Lister, D. (2020). Version 4 of the CRU TS monthly high-resolution gridded multivariate climate dataset. *Scientific Data*, *7*(1), 109. https://doi.org/10.1038/s41597-020-0453-3

Hoekstra, A., Chapagain, A. K., Aldaya, M. M., & Mekonnen, M. M. (2012). *The water footprint assessment manual: Setting the global standard*. Routledge.

Hoekstra, A. Y., & Hung, P. Q. (2003). *Virtual water trade*. *12*, 1–244.

Howarth, R. W., & Jacobson, M. Z. (2021). How green is blue hydrogen? *Energy Science & Engineering*, *9*(10), 1676–1687.

Hydrogen Council. (2023). *Hydrogen Insights 2023: An update on the state of the global hydrogen economy, with a deep dive into North America*. https://hydrogencouncil.com/wp-content/uploads/2023/05/Hydrogen-Insights-2023.pdf

IEA. (2000). *World Energy Outlook, 1999, IEA, Paris*. https://www.iea.org/reports/world-energy-outlook-1999

IEA. (2019). *The future of Hydrogen*. IEA, Paris. https://www.iea.org/reports/the-future-of-hydrogen

IEA. (2021). Net zero by 2050: A roadmap for the global energy sector. *IEA: Paris, France*. https://www.iea.org/reports/net-zero-by-2050

IEA. (2022a). *Global Hydrogen Review 2022*. IEA. https://www.iea.org/reports/global-hydrogen-review-2022

IEA. (2022b). *Hydrogen Projects Database*. https://www.iea.org/reports/hydrogen-projects-database

Incer-Valverde, J., Korayem, A., Tsatsaronis, G., & Morosuk, T. (2023). "Colors" of hydrogen: Definitions and carbon intensity. *Energy Conversion and Management*, *291*, 117294. https://doi.org/10.1016/j.enconman.2023.117294

Iribarren, D., Susmozas, A., Petrakopoulou, F., & Dufour, J. (2014). Environmental and exergetic evaluation of hydrogen production via lignocellulosic biomass gasification. *Journal of Cleaner Production*, *69*, 165–175. https://doi.org/10.1016/j.jclepro.2014.01.068

Jack, J., Zhu, W., Avalos, J. L., Gong, J., & Ren, Z. J. (2021). Anode co-valorization for scalable and sustainable electrolysis. *Green Chem.*, *23*(20), 7917–7936. https://doi.org/10.1039/D1GC02094C

Jiang, J., Lopez-Ruiz, J. A., Bian, Y., Sun, D., Yan, Y., Chen, X., Zhu, J., May, H. D., & Ren, Z. J. (2023). Scale-up and techno-economic analysis of microbial electrolysis cells for hydrogen production from wastewater. *Water Research*, *241*, 120139. https://doi.org/10.1016/j.watres.2023.120139

Kırtay, E. (2011). Recent advances in production of hydrogen from biomass. *Energy Conversion and Management*, *52*(4), 1778–1789. https://doi.org/10.1016/j.enconman.2010.11.010

Lampert, D. J., Cai, H., Wang, Z., Keisman, J., Wu, M., Han, J., Dunn, J., Sullivan, J. L., Elgowainy, A., & Wang, M. (2015). *Development of a life cycle inventory of water consumption associated with the production of transportation fuels*. Argonne National Lab.(ANL), Argonne, IL (United States).

Lee, U., Xu, H., Daystar, J., Elgowainy, A., & Wang, M. (2019). AWARE-US: Quantifying water stress impacts of energy systems in the United States. *Science of The Total Environment*, *648*, 1313–1322. https://doi.org/10.1016/j.scitotenv.2018.08.250

Macknick, J., Newmark, R., Heath, G., & Hallett, K. (2011). Review of operational water consumption and withdrawal factors for electricity generating technologies. *Environmental Research Letters*.

Macknick, J., Sattler, S., Averyt, K., Clemmer, S., & Rogers, J. (2012). The water implications of generating electricity: Water use across the United States based on different electricity pathways through 2050. *Environmental Research Letters*, *7*(4), 045803.

Mehmeti, A., Angelis-Dimakis, A., Arampatzis, G., McPhail, S. J., & Ulgiati, S. (2018). Life Cycle Assessment and Water Footprint of Hydrogen Production Methods: From Conventional to Emerging Technologies. *Environments*, *5*(2). https://doi.org/10.3390/environments5020024

Mekonnen, M. M., Gerbens-Leenes, P. W., & Hoekstra, A. Y. (2015). The consumptive water footprint of electricity and heat: A global assessment. *Environ. Sci.: Water Res. Technol.*, *1*(3), 285–297. https://doi.org/10.1039/C5EW00026B

Mekonnen, M. M., & Hoekstra, A. Y. (2011). The green, blue and grey water footprint of crops and derived crop products. *Hydrology and Earth System Sciences*, *15*(5), 1577–1600.

Mekonnen, M. M., & Hoekstra, A. Y. (2012). The blue water footprint of electricity from hydropower. *Hydrology and Earth System Sciences*, *16*(1), 179–187. https://doi.org/10.5194/hess-16-179-2012

Meldrum, J., Nettles-Anderson, S., Heath, G., & Macknick, J. (2013). Life cycle water use for electricity generation: A review and harmonization of literature estimates. *Environmental Research Letters*, *8*(1), 015031.

Mielke, E., Anadon, L. D., & Narayanamurti, V. (2010). Water consumption of energy resource extraction, processing, and conversion. *Belfer Center for Science and International Affairs*.

588 Molden, D. (2013). *Water for food water for life: A comprehensive assessment of water management in*
589 *agriculture*. Routledge.

590 Mulder, K., Hagens, N., & Fisher, B. (2010). Burning water: A comparative analysis of the energy return on
591 water invested. *Ambio*, *39*, 30–39.

592 Osselin, F., Soulaine, C., Fauguerolles, C., Gaucher, E. C., Scaillet, B., & Pichavant, M. (2022). Orange
593 hydrogen is the new green. *Nature Geoscience*, *15*(10), 765–769.
594 https://doi.org/10.1038/s41561-022-01043-9

595 Paulot, F., Paynter, D., Naik, V., Malyshev, S., Menzel, R., & Horowitz, L. W. (2021). Global modeling of
596 hydrogen using GFDL-AM4.1: Sensitivity of soil removal and radiative forcing. *International*
597 *Journal of Hydrogen Energy*, *46*(24), 13446–13460.
598 https://doi.org/10.1016/j.ijhydene.2021.01.088

599 Penev, M. (2022a). Hydrogen Analysis Production Models. *Current Central Hydrogen Production from*
600 *Steam Methane Reforming (SMR) of Natural Gas with CO2 Sequestation*.
601 https://www.nrel.gov/hydrogen/assets/docs/current-central-steam-methane-reforming-with-
602 co2-sequestration-version-aug-22.xlsm

603 Penev, M. (2022b). Hydrogen Analysis Production Models. *Current Central Hydrogen Production from*
604 *Steam Methane Reforming (SMR) of Natural Gas without CO2 Sequestration.*
605 https://www.nrel.gov/hydrogen/assets/docs/current-central-steam-methane-reforming-
606 without-co2-sequestration-version-aug22.xlsm

607 Penev, M. (2022c). Hydrogen Analysis Production Models. *Current Central Hydrogen Production from*
608 *Coal Gasification with CO_2 Capture and Sequestration*.
609 https://www.nrel.gov/hydrogen/assets/docs/current-central-coal-gasification-with-co2-
610 sequestration-version-aug22.xlsm

611 Porporato, A., & Yin, J. (2022). *Ecohydrology: Dynamics of Life and Water in the Critical Zone*.
612 https://doi.org/10.1017/9781108886321

613 Postle, M., George, C., Upson, S., Hess, T., & Morris, J. (2012). Assessment of the efficiency of the water
614 footprinting approach and of the agricultural products and foodstuff labelling and certification
615 schemes. *Report for the European Commission, DG Environment*.

Power, H. (2005). Reclamation Managing Water in the West. *Power Resource Office—US Department of Interior, Bureau of Reclamation: Washington, DC, USA*.

Ritchie, H., Roser, M., & Rosado, P. (2022). *Energy*. https://ourworldindata.org/energy

Rosa, L., Chiarelli, D. D., Rulli, M. C., Dell'Angelo, J., & D'Odorico, P. (2020). Global agricultural economic water scarcity. *Science Advances*, *6*(18), eaaz6031. https://doi.org/10.1126/sciadv.aaz6031

Rosa, L., Sanchez, D. L., Realmonte, G., Baldocchi, D., & D'Odorico, P. (2021). The water footprint of carbon capture and storage technologies. *Renewable and Sustainable Energy Reviews*, *138*, 110511. https://doi.org/10.1016/j.rser.2020.110511

Rousseau, R., Etcheverry, L., Roubaud, E., Basséguy, R., Délia, M.-L., & Bergel, A. (2020). Microbial electrolysis cell (MEC): Strengths, weaknesses and research needs from electrochemical engineering standpoint. *Applied Energy*, *257*, 113938. https://doi.org/10.1016/j.apenergy.2019.113938

Ruiz, H., Sunarso, A., Ibrahim-Bathis, K., Murti, S., & Budiarto, I. (2020). GIS-AHP Multi Criteria Decision Analysis for the optimal location of solar energy plants at Indonesia. *Energy Reports*, *6*, 3249–3263.

Rutkowski, M., & Darlene, S. (2008). H2A hydrogen production models. *Current (2005) Hydrogen from Coal without CO2 Capture and Sequestration*. https://view.officeapps.live.com/op/view.aspx?src=https%3A%2F%2Fwww.nrel.gov%2Fhydrogen%2Fassets%2Fdocs%2Fcurrent-central-coal-without-co2-sequestration-v2-1-1.xls&wdOrigin=BROWSELINK

Salkuyeh, Y. K., Saville, B. A., & MacLean, H. L. (2018). Techno-economic analysis and life cycle assessment of hydrogen production from different biomass gasification processes. *International Journal of Hydrogen Energy*, *43*(20), 9514–9528.

Sand, M., Skeie, R. B., Sandstad, M., Krishnan, S., Myhre, G., Bryant, H., Derwent, R., Hauglustaine, D., Paulot, F., Prather, M., & Stevenson, D. (2023). A multi-model assessment of the Global Warming Potential of hydrogen. *Communications Earth & Environment*, *4*(1), 203. https://doi.org/10.1038/s43247-023-00857-8

643 Spang, E. S., Moomaw, W. R., Gallagher, K. S., Kirshen, P. H., & Marks, D. H. (2014). The water
644 consumption of energy production: An international comparison. *Environmental Research*
645 *Letters*, *9*(10), 105002. https://doi.org/10.1088/1748-9326/9/10/105002

646 Susmozas, A., Iribarren, D., Zapp, P., Linβen, J., & Dufour, J. (2016). Life-cycle performance of hydrogen
647 production via indirect biomass gasification with CO2 capture. *International Journal of Hydrogen*
648 *Energy*, *41*(42), 19484–19491.

649 Togni, L., & Fakoury, R. (2022). *Regional Insights into Low-carbon Hydrogen Scale Up: World Energy*
650 *Insights Working Paper*.

651 Tonelli, D., Rosa, L., Gabrielli, P., Caldeira, K., Parente, A., & Contino, F. (2023). Global land and water
652 limits to electrolytic hydrogen production using wind and solar resources. *Nature*
653 *Communications*, *14*(1), 5532. https://doi.org/10.1038/s41467-023-41107-x

654 Tuninetti, M., Tamea, S., D'Odorico, P., Laio, F., & Ridolfi, L. (2015). Global sensitivity of high-resolution
655 estimates of crop water footprint. *Water Resources Research*, *51*(10), 8257–8272.

656 UNECE. (2021). *Technology Brief Hydrogen.* United Nations Economic Comission for Europe Task Force on
657 Hydrogen, Geneva. https://unece.org/sites/default/files/2021-
658 10/Hydrogen%20brief_EN_final_0.pdf

659 UNEP. (2021). *Progress on Integrated Water Resources Management. Tracking SDG 6 series: Global*
660 *indicator 6.5.1 updates and acceleration needs*. https://www.sdg6data.org/en/indicator/6.5.1

661 Vallino, E., Ridolfi, L., & Laio, F. (2020). Measuring economic water scarcity in agriculture: A cross-country
662 empirical investigation. *Environmental Science & Policy*, *114*, 73–85.

663 Vallino, E., Ridolfi, L., & Laio, F. (2021). Trade of economically and physically scarce virtual water in the
664 global food network. *Scientific Reports*, *11*(1), 22806. https://doi.org/10.1038/s41598-021-
665 01514-w

666 Vanham, D., & Bidoglio, G. (2013). A review on the indicator water footprint for the EU28. *Ecological*
667 *Indicators*, *26*, 61–75.

668 Wu, M., Mintz, M., Wang, M., & Arora, S. (2009). Water consumption in the production of ethanol and
669 petroleum gasoline. *Environmental Management*, *44*, 981–997.

Zarrouk, S. J., & Moon, H. (2014). Efficiency of geothermal power plants: A worldwide review. *Geothermics*, *51*, 142–153. https://doi.org/10.1016/j.geothermics.2013.11.001

Zoghi, M., Ehsani, A. H., Sadat, M., javad Amiri, M., & Karimi, S. (2017). Optimization solar site selection by fuzzy logic model and weighted linear combination method in arid and semi-arid region: A case study Isfahan-IRAN. *Renewable and Sustainable Energy Reviews*, *68*, 986–996.